Residual Stress Generation in Tungsten-Copper Brazed Joint Using Brazing Alloy

D. Easton[1], J. Wood[1], S. Rahimi[2], A. Galloway[1], Y. Zhang[1], C. Hardie[3]
[1] Mechanical and Aerospace Engineering, University of Strathclyde, Glasgow, United Kingdom
[2]Advanced Forming Research Centre, University of Strathclyde, Glasgow, United Kingdom
[3]Material Research Laboratory, Culham Centre for Fusion Energy, Oxfordshire, United Kingdom

***Abstract*— Understanding the residual stress state in brazed joints is crucial for operational design and life time performance of the part in service. High magnitude residual stresses are expected in the joined materials following cooling from brazing temperatures (≈950C) due to large mismatches in material properties such as coefficient of thermal expansion and Young's modulus (E). This paper aims to further understanding of the residual stresses caused when brazing tungsten to copper using a eutectic gold-copper brazing alloy. This configuration is potentially useful for future divertor designs. Finite Element Analysis (FEA) has been used to predict the brazing induced stresses and residual stress measurements were carried out on the brazed joint by X-ray diffraction (XRD) to validate the prediction model. Large residual stresses are predicted and measured in the tungsten; however there is disagreement in the nature of the stress. Predicted stresses are highly tensile in nature close to the brazing interface, whereas the measured stresses are highly compressive. The disagreement is believed to be caused by the model not accurately simulating the complex brazing process. Residual stress measurements on the copper were not possible due to texturing during brazing, grain growth and significant inelastic strains. Misalignment of parent materials was also observed to significantly affect residual stresses.**

Keywords — residual stress; tungsten; x-ray diffraction; brazing

I. INTRODUCTION

Tungsten has been proposed as potential armour material in high heat flux components such as the divertor in a future thermonuclear fusion demonstration reactor (DEMO)[1-4]. The divertor will undergo standard heat loads from 10MW/m^2 up to 20MW/m^2 during plasma instabilities[5]. Tungsten has been identified as an armour material as it has the highest melting point of all metals[6], good thermal performance and erosion resistance[7, 8]. However, tungsten is brittle in nature at lower temperatures and as such is not suitable as a structural material. A popular solution is to bond tungsten with an appropriate structural material with high thermal conductivity and capacity such as copper[9] that has excellent thermal performance and ductility (386W/mK at room temperature [10]).). However, there are extremely high dissimilarities in the thermal and mechanical properties between tungsten, copper and gold-copper brazing alloy [11]. A suitable dissimilar material joining process that can be used to bond tungsten and copper is vacuum furnace brazing with the use of an interlayer [11, 12].

The existing material property mismatches leads to the generation of residual stress in a dissimilar material butt jointed component in addition to the thermally induced residual stresses [13-16]. Residual stresses are elastic in nature and self-equilibrating, and in the case of a dissimilar material brazed joint are caused by constraint on differential contraction during cooling in the parent materials and brazing alloy[17, 18]. In the case of a tungsten, gold-copper and copper brazed joint, the copper and gold-copper will want to contract much more than the tungsten due a much higher coefficient of thermal expansion (CTE). This induces local inelastic strains in the materials as there is restraint on contraction as the braze solidifies and cools. Once the load has been removed i.e. $\Delta T=0$, elastic springback occurs and permanent elastic residual stresses remain in the materials. The extent and nature of these stresses is highly dependent on the properties of the parent materials and brazing material[19]. The free edge of the component is an area with a theoretical singularity in elastic stress[20]. Tensile axial residual stresses are expected in the tungsten and compressive stresses in the copper based on previous theoretical work[14].

II. EXPERIMENTAL

A. *Specimen design and fabrication*

Tungsten-gold/copper-copper (W-AuCu-Cu) brazed specimens were fabricated in a simple butt joint arrangement for the purpose of measuring residual stresses. Each specimen consisted of 2 parent material components, one pure W rod and one oxygen free high conductivity (OFHC) Cu rod, with dimensions 25mm length x 12.7mmØ. These were vacuum brazed with a eutectic Au Cu (Au80%wt – Cu20%wt) brazing alloy interlayer with thickness 50µm. An example of a brazed W-AuCu-Cu specimen can be seen in Figure1.

The brazing procedures and parameters were chosen following previous research by the authors [11, 12]. Following machining, cleaning and jigging in accordance with [11], the specimens were brazed in a vacuum furnace. Brazing was performed at 950°C and cooled at a rate no greater than 10°C/min.

X-Ray Diffraction

Residual stress measurements were performed using a Proto Manufacturing LXRD machine[21]. A photo of the setup can be seen in Figure 2. Measuring residual stresses by X-ray diffraction (XRD) is an established technique by which the elastic strain in a material is calculated and residual stress evaluated using elastic constants[22]. X-rays are fired onto a sample, of which some will be diffracted due to interaction with the crystalline lattice of the sample. A series of calculations stemming from Bragg's Law are then used to calculate the strain and stress.

$$n\lambda = 2d'sin\theta$$

Where λ is the wavelength of the x-ray, d' is the inter-planar spacing (d-spacing) and θ is the angular position of the diffraction lines.

Measurements were taken on the W and Cu. Readings were taken at multiple circumferential orientations (0°, 90°, 180° and 270°) on 5 samples. At each orientation, multiple axial locations were measured using a 1mm diameter aperture as shown in the schematic in Figure 3. The locations of the measurements were biased towards the interface. The highest discontinuity stresses and stress gradients were expected in this region due to the dissimilarity of the materials as was shown to be the case in similar previous studies [15, 23].

The stress and measurement uncertainty was obtained from the best fit to the $sin^2\psi$ plot[22]. The residual stresses were measured in two perpendicular directions: Axial, along the length of the rod ($\varphi = 0^\circ$) and Hoop, perpendicular to its lengths ($\varphi = 90^\circ$).. An illustration of the various reference frames for XRD measurements can be found in Figure 4[22].

The stresses in the tungsten part were calculated from the strains of the 222 Bragg reflection using Co Kα radiation, assuming elastic properties of E =400606 MPa and Poisson's ratio of $\nu = 0.285$.

III. MODELLING

A Finite Element Analysis (FEA) was performed to predict the residual stress state in the bonded component following cooling from the brazing temperature. In order to accurately simulate the material behaviour during the thermal process, temperature dependant material properties are required for the three materials. These properties are not currently available for the AuCu brazing alloy. Work by the author is on-going in producing thermal and mechanical properties from room temperature to brazing temperature using experimental testing including tensile testing at elevated temperatures, Simultaneous Thermal Analysis (STA) and dilatometer tests.

Material	Temp(°C)	CTE x10^{-6} (/K)	K (W/mK)	E (GPA)	Yield Stress (MPa)	E_{tan} (GPA)	ρ (kg/m^3)	ν
AgCu	20	15.3	493	59.2	170	30	10100	0.37
	778	16	404	1	1	1	10100	0.37
Copper	20	16.7	387	126	40	12.6	8940	0.33
	778	18.8	348	80	6.4	8	8556	0.33
Tungsten	20	4.4	173	399	1296	39.9	19300	0.28
	778	4.8	116	365	625	36.5	19090	0.29

Table 1 - Material properties used for FEA

Due to the lack of data for the brazing alloy, a material model for a different alloy has been used for the simulation. Hamilton et al [15] produced data for a silver/copper alloy (Ag72% - Cu28%). Due to the relatively similar properties of gold and silver such as elastic modulus at room temperature of 79Gpa and 83GPa respectively, the similar balance of copper in each alloy and the similar known properties for each alloy (CTE, at room temperature for AuCu= 17.9x10^{-6}/°C [24] and AgCu=15.317.9x10^{-6}/°C [15]) it was believed that the FEA results should be representative of the actual W-AuCu-Cu configuration. In particular because the FEA analysis considers the material as continuum and the microstructure and crystal plasticity effects have not been taken into account. A summary of the room temperature and braze temperature material properties can be found in Table 1. A bilinear kinematic hardening law was used for post yield behaviour.

The FE model was performed using ANSYS 15 [25]. A 2D axisymmetric static structural model was used which assumes perfect alignment of component parts. An initial stress free state at brazing temperature is applied. The thermal conditions applied were T_{braze}=778°C and T_{room}=20°C. As the cooling rate was very slow (less than 10°C/min) , thermal gradients are negligible so a steady state analysis is valid [13, 26]. Stresses have been considered in the axial and circumferential directions. The primary element type used was 8 node quadrilateral PLANE182 elements with 4 elements across the thickness of the braze which was shown to be sufficient in a previous convergence study[27]. The predicted residual stress results at the free edge of the component can be found in Figure 5. The edge of the tungsten away from the braze interface is at position y=0mm, with y>0 as the braze layer is approached.

High tensile axial residual stresses are found in the tungsten near the braze interface. The magnitude of the stress increases with proximity to the braze layer, with a maximum of about 1000MPa. This finding is comparable to previous studies [15, 26], with the tensile stresses occurring in the high E, low CTE component and compressive residual stresses found in the low E, high CTE material. This is to be expected due to the constraint on differential contraction during cooling as explained in section 1. Tensile circumferential stresses occur in over an extremely small area in the tungsten close to the braze, with a maximum magnitude of about 200MPa. Circumferential stresses in the copper are compressive away from the braze and tensile close to the interface.

IV. RESULTS AND DISCUSSION

A. XRD residual stress results - Tungsten

The axial and circumferential residual stresses in tungsten as measured by XRD can be found in Figure 6 and Figure 7 respectively. Considering the axial stress results from Figure 6, it can be seen that for the majority of measurements there is a clear trend with high compressive residual stresses close to the braze interface. These stresses sharply decrease at 0.5-1mm distance from the interface. It was predicted that this is the region where the highest stresses occur, however the compressive nature of the stresses are in conflict

with those predicted by FEA. Due to the large volume of measurements taken, it is believed that the opposite sign of stress cannot be attributed to measurement or set up errors. The large magnitude of stresses near the brazed layer was expected as the yield stress of tungsten is very high. This allows high elastic stresses to occur in the tungsten without any plastic deformation. Conversely, copper was expected to undergo plastic deformation. The stresses caused by the material property dissimilarity of tungsten, copper and the braze alloy were sufficiently high resulting in yielding and a large degree of plastic deformation.

Figure 7shows the circumferential stresses measured in the tungsten side of each sample. Large compressive residual stresses are found in the region close to the braze layer, similar to the axial stresses. Again, these are different in sign than predicted by FEA. As with the FE predictions and axial measurements, at a distance of3-5mm from the braze the stresses drop to a level around 0MPa ±100MPa.

It is not however believed that the lower temperature and differing material model could cause the fundamental difference in the nature of the stress (high tensile predicted/high compressive measured). This has been attributed to the FE model not being sufficiently able to capture the complex behaviour that occurs during the cooling process with the model currently being used. At temperatures close to the brazing temperature, multiple processes are occurring which can affect residual stress including; inter diffusion of parent materials and brazing material, geometrical misalignment, differing amounts of thermal contraction, recrystallization, phase transformation and heterogeneous thermally induced plastic deformation. A limitation of XRD is that measurements are only describing the stress at the surface as x-ray penetration is limited to about 5 microns[22]. The stresses deeper into the material are not known at this point. Another limitation of the current technology is that a compromise must be made between spatial resolution and accuracy. Increasing the spot size of the measurement was found to result in a stronger diffraction peak. However, this reduced the ability to measure stresses at specific points. The larger aperture also acted to blunt the stress results in highly stressed areas, as with the larger diameter area of interest (2mm as opposed to 1mm), there was a significant portion of lesser stressed material which reduced the average for the area.

To better understand the complex metallurgical condition and stress field close to the braze interface a multifaceted approach is necessary. Further FEA is required to investigate the many variables that could be causing the lack of correlation between FE predictions and experimentally measured results. It has been shown that factors such as axial and angular misalignment and fillet radii can play a significant role in the singularity and therefore stress field at a region of geometrical and material discontinuity[28]. On-going work to characterise the AuCu brazing alloy will provide more accurate results. Experimentally, different residual stress measurement techniques shall be applied to confirm the XRD measurements, and to better understand the stress filed through the thickness. Electronic speckle pattern interferometry (ESPI) hole drilling is proposed as a method for residual stress measurement. Electron back scatter diffraction (EBSD) shall also be utilised to analyse microstructure character distribution such as local lattice misorientations, micro-texture and recrystallization behaviour in the complex braze interfacial region.

B. XRD residual stress results - Copper

XRD measurements on the post-braze copper material proved to be unreliable. The errors associated with curve fitting to measured peaks were too great to be considered valid. There are a few reasons why this has occurred. Measurements can be degraded due to texturing of the material (copper) during the brazing process, and grain sizes >100µm result in fewer grains contributing to the diffraction peak hence a less accurate result[22]. Another source of error is due to the plastic deformation and inelastic strains present in the copper. This can cause distortions within the lattice, and hence affect d-spacing and XRD results. As the material property mismatch is very significant for tungsten compared to the braze alloy and copper (see Table 1), large discontinuity stresses were expected. In easily yielding copper, this has resulted in plastic deformation and strains. During plastic deformation, grains undergo shear stresses causing skewed lattices which negatively affect the Bragg Law calculations. Also, in regions with plastic deformation, the peaks

from highly elastically stressed grains are coincided on those from stress free grains causing deviation from Gaussian/Pearson distribution. This causes inaccuracies in measured results[22].
To overcome these issues, ESPI hold drilling shall be used to measure stresses and EBSD used to better understand the elastic and inelastic strains present in the copper.

C. Effects of misalignment on residual stresses

It can be seen from Figure 6, sample B has largely varying axial stresses in the tungsten at equal positions from the interface depending on circumferential position. At a distance of 0.5mm from the interface, the axial stress at 0 degrees is a small tensile stress of 27MPa. At the opposite side of the material at 170 degrees (measurements were not performed at 180 degrees on this sample due to a surface flaw) the stress is significantly higher at 236MPa compressive. Figure 8 shows the visually noticeable misalignment in the sample. The degree of misalignment is particularly noticeable when viewed in an SEM. Measurements using a computer-measuring machine (CMM) will quantify the degree of misalignment. The high stress (at 170 degrees) occurs in the area of the sample that is more constrained by the other materials. The very low stress occurs at the edge of the tungsten (at 0 degrees) that is offset from the copper. This is a logical result as the tungsten that is offset from the copper is essentially free to contract during cooling without any constraint.

V. CONCLUSIONS

This study has predicted the residual stresses that form in a tungsten to copper brazed component with eutectic gold-copper interlayer due to material property dissimilarity using FEA and measured the stresses in a real component using XRD. The following conclusions have been made:

- Due to significant dissimilarity in material properties combined with other factors such as geometrical discontinuities, large residual stresses are expected in the parent materials near the braze interface.
- FEA predicts highly tensile axial stresses in the tungsten and lesser compressive stresses in the copper. This is in agreement with previous experimental trends and theoretical understanding. These results are for a W-AgCu-Cu sample, which while not identical to the AuCu sample in reference, it should behave relatively similar.
- High tensile circumferential stresses are also predicted in the tungsten. These are very localised to the braze interface.
- Experimental results obtained by XRD show that the tungsten is in a highly compressive stress state near the interface, both axially and circumferentially. This is not in agreement with current modelling efforts. Further residual stress measurements using ESPI is planned, which will validate the XRD results.
- A continuation of work to characterise AuCu brazing alloy temperature dependant material properties will lead to better agreement
- XRD measurement on post-braze copper was not possible due to a number of factors including texturing, grain size, plastic strains and deformation.
- Axial misalignment has been shown to have a very significant effect on the free edge stress field in a dissimilar material brazed component.

REFERENCES

[1] P. Norajitra, R. Giniyatulin, T. Ihli, G. Janeschitz, W. Krauss, R. Kruessmann, *et al.*, "He-cooled divertor development for DEMO," *Fusion Engineering and Design*, vol. 82, pp. 2740-2744, 2007.

[2] M. Kaufmann and R. Neu, "Tungsten as first wall material in fusion devices," *Fusion Engineering and Design*, vol. 82, pp. 521-527, 2007.

[3] P. Norajitra, S. I. Abdel-Khalik, L. M. Giancarli, T. Ihli, G. Janeschitz, S. Malang, *et al.*, "Divertor conceptual designs for a fusion power plant," *Fusion Engineering and Design*, vol. 83, pp. 893-902, 2008 2008.

[4] A. Li-Puma, M. Richou, P. Magaud, M. Missirlian, E. Visca, and V. P. Ridolfini, "Potential and limits of water cooled divertor concepts based on monoblock design as possible candidates for a DEMO reactor," *Fusion Engineering and Design*, vol. 88, pp. 1836-1843, 2013.

[5] D. Maisonnier, I. Cook, S. Pierre, B. Lorenzo, D. P. Luigi, G. Luciano, *et al.*, "DEMO and fusion power plant conceptual studies in Europe," *Fusion Engineering and Design*, vol. 81, pp. 1123-1130, 2006.

[6] Erik Lassner and W.-D. Schubert, Tungsten- Properties, Chemistry, Technology of the Element, Alloys, and Chemical Compounds 1999.

[7] H. Bolt, V. Barabash, W. Krauss, J. Linke, R. Neu, S. Suzuki, *et al.*, "Materials for the plasma-facing components of fusion reactors," *Journal of Nuclear Materials*, vol. 329-333, pp. 66-73, 2004.

[8] M. Rieth and e. al, "Recent progress in research on tungsten materials for nuclear fusion applications in Europe," *Journal of Nuclear Materials*, vol. 432, pp. 482-500, 2013 2013.

[9] J. Reiser and M. Rieth, "Optimization and limitations of known DEMO divertor concepts," *Fusion Engineering and Design*, vol. 87, pp. 718-721, 2012.

[10] JAHM. Software", "Material Property Database (MPDB)," ed, 2015. (accessed 20/05/15)

[11] D. Easton, J. Wood, A. Galloway, Y. Zhang, M. B. O. Robbie, and C. Hardie, "Brazing Development and Interfacial Metallurgy Study of Tungsten and Copper Joints with Eutectic Gold Copper Brazing Alloy," *Fusion Engineering and Design*, vol. In Press.

[12] Y. Zhang, A. Galloway, J. Wood, M. B. O. Robbie, D. Easton, and W. Zhu, "Interfacial metallurgy study of brazed joints between tungsten and fusion related materials for divertor design," *Journal of Nuclear Materials*, vol. 454, pp. 207-216, 2014.

[13] N. Hamilton, "Niall Hamilton Thesis Master," PhD, Mechanical and Aerospace Engineering, University of Strathclyde, 2013.

[14] N. R. Hamilton, J. Wood, A. Galloway, M. B. Olsson Robbie, and Y. Zhang, "The metallurgy, mechanics, modelling and assessment of dissimilar material brazed joints," *Journal of Nuclear Materials*, vol. 432, pp. 42-51, 2013.

[15] N. R. Hamilton, J. Wood, D. Easton, M. B. O. Robbie, Y. Zhang, and A. Galloway, "Thermal autofrettage of dissimilar material brazed joints," *Materials & Design*, vol. 67, pp. 405-412, 2015.

[16] Y. Nemoto, "Analysis and measurement of residual stress distribution of vanadium/ceramics joints for fusion reactor applications," *Journal of Nuclear Materials*, vol. 258-263 1998.

[17] P. J. Withers and H. K. D. H. Bhadeshia, "Residual Stress Part 1, Measurement and Techniques," *Materials Science and Technology*, vol. 17, p. 335, 2001.

[18] P. J. Withers and H. K. D. H. Bhadeshia, "Residual Stress Part 2, Natrue and Origins," *Materials Science and Technology*, vol. 17, p. 366, 2001.

[19] P. Dadras, J. M. Ting, and M. L. Lake, "Brazing residual stresses in Glidcop-All2Si-Be," *Journal of Nuclear Materials*, vol. 230, pp. 164-172, 1996.

[20] P. Kelly, "The design of joints between elastically dissimilar components," *Journal of Strain Analysis*, vol. 27, pp. 15-20, 1992.

[21] http://www.protoxrd.com/lxrd-laboratory.html. (accessed 20/05/15)

[22] M. E. e. a. Fitzpatrick. Determination of Residual Stresses by X-ray Diffraction. *(Issue 2)*.

[23] S.-B. Lee, "Finite-element ana!ysis and X-ray measuremznt of the residual stresses of ceramic/metal joints," *Journal of Materials Processing Technology*, vol. 67, pp. 167-172, 1997.

[24] *http://www.wesgometals.com/resources/mechanical-physical-properties/*. (accessed 20/05/15)

[25] http://www.ansys.com/. (accessed 20/05/15)

[26] M. Galli, J. Botsis, J. Janczak-Rusch, G. Maier, and U. Welzel, "Characterization of the Residual Stresses and Strength of Ceramic-Metal Braze Joints," *Journal of Engineering Materials and Technology*, vol. 131, p. 021004, 2009.

[27] T. Peat, "An Investigation into the Modelling of Dissimilar Material Joints and the Application of Autofrettage to Reduce Residual Stresse," University of Strathclyde, 2012.

[28] J. Wood and e. al, "Theoretical elastic stress singularities...much maligned and misunderstood," *NAFEMS World Congress 2015*, 2015

Figure 1 – Brazed W-AuCu-Cu specimen

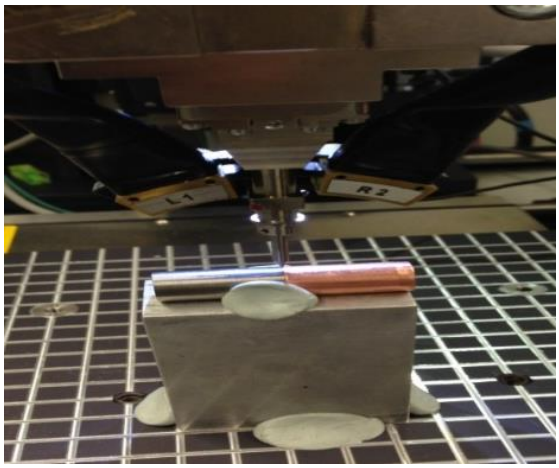
Figure 2 - XRD set up

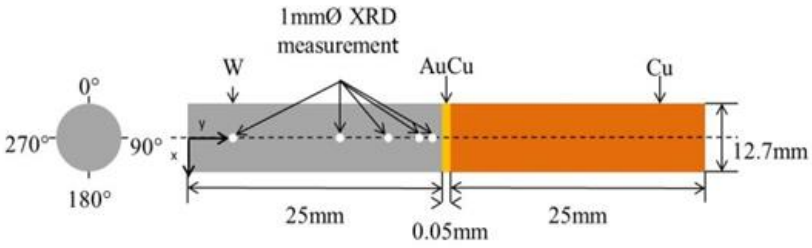

Figure 3 - Residual stress measurement positions on tungsten component. Left: circumferential orientation. Right: axial position and dimensions

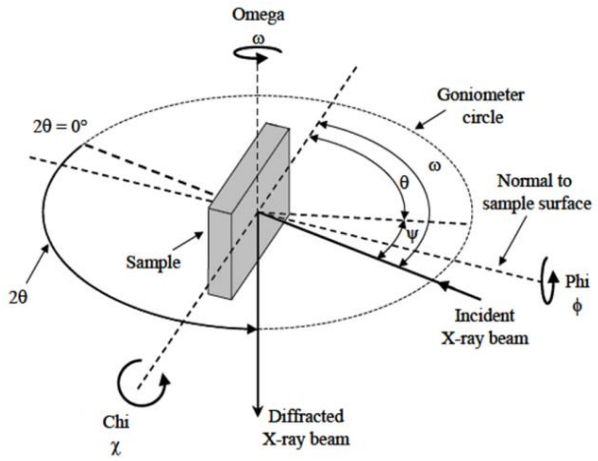

Figure 4 – XRD angles and rotations

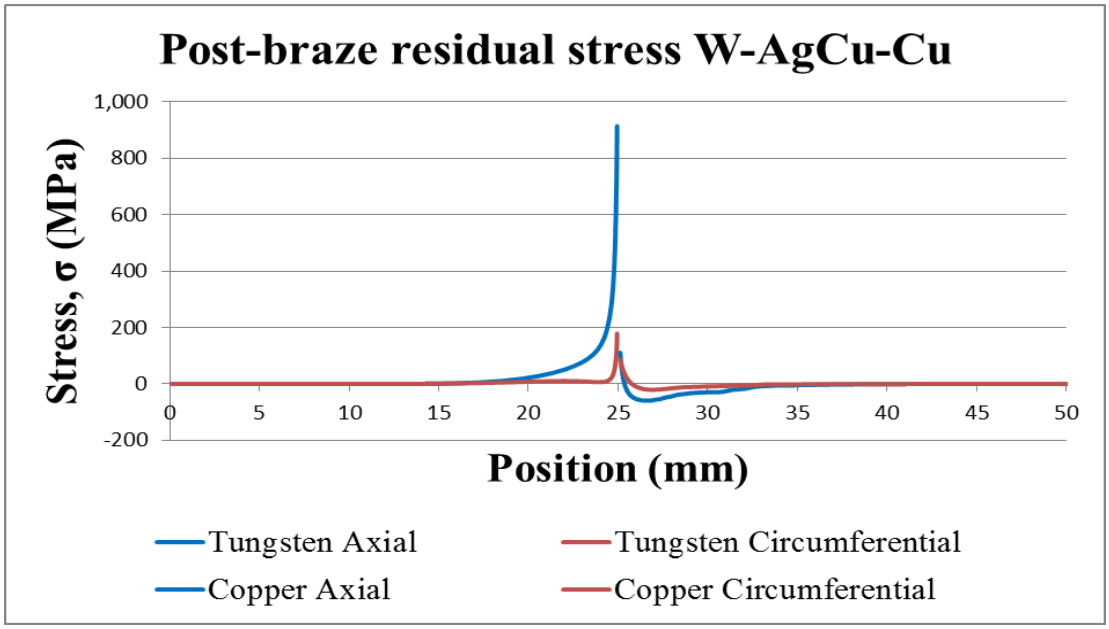

Figure 5 - FEA predicted residual stress in W-AgCu-Cu

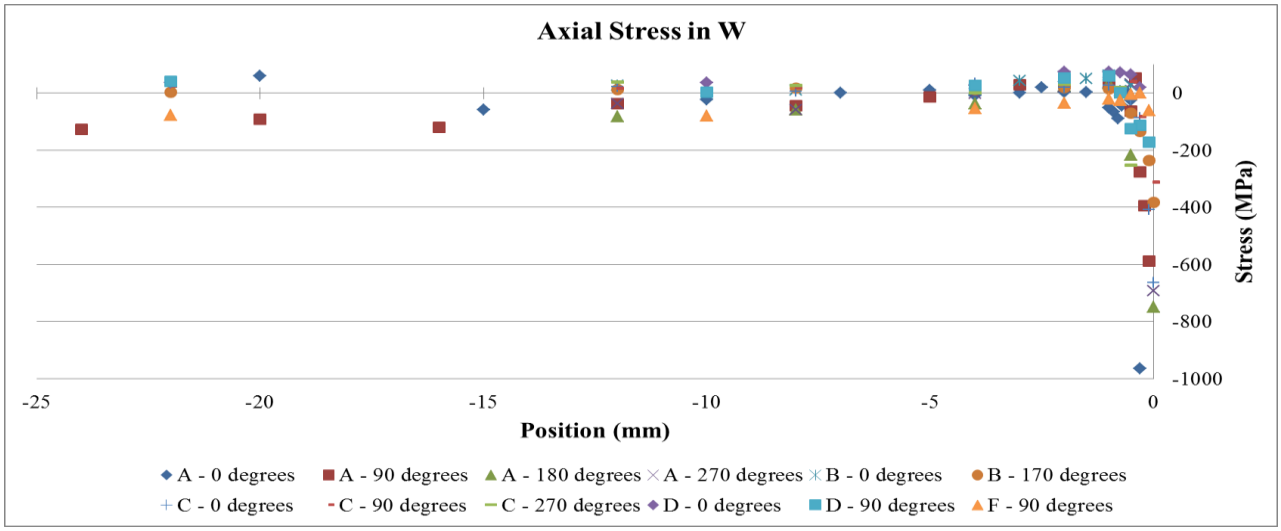

Figure 6 - Tungsten axial stress XRD measurements

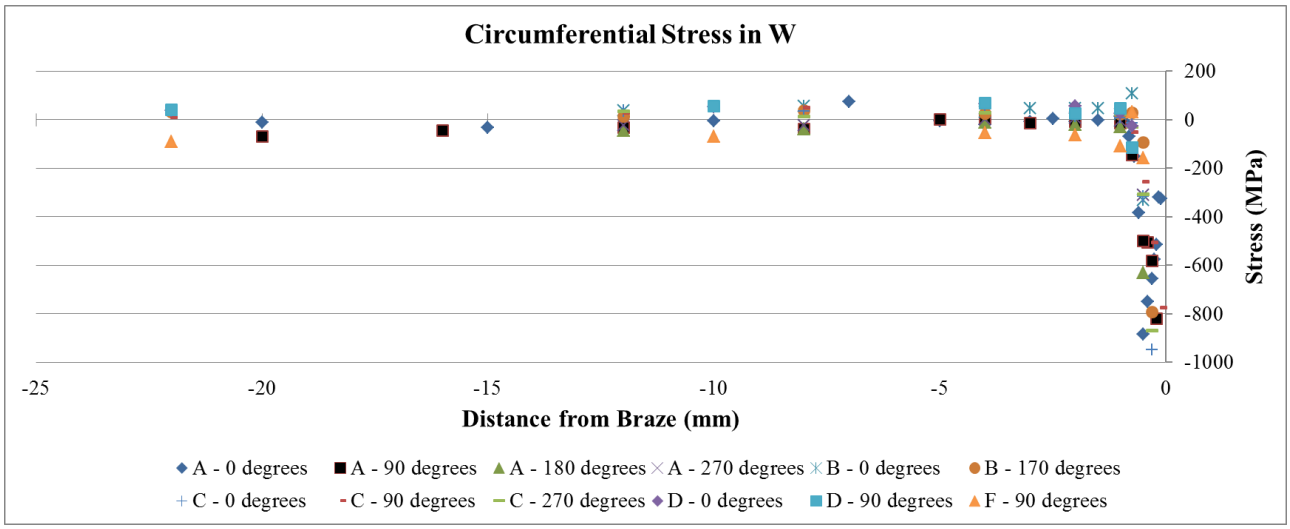

Figure 7 - Tungsten circumferential stress XRD measurements

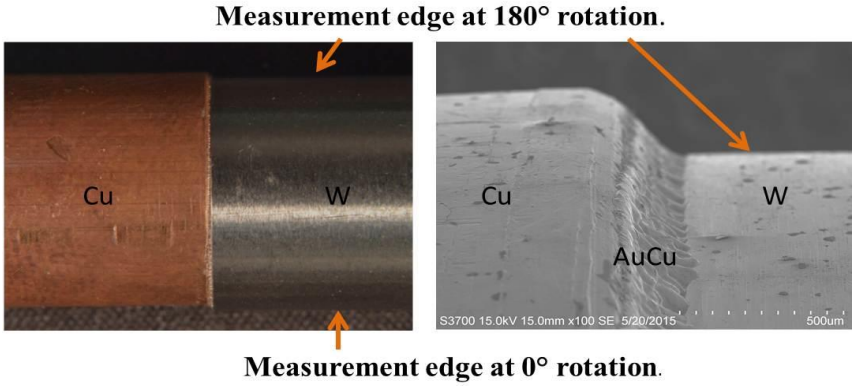

Figure 8 – Sample B axial misalignment - Left: Photograph Right: SEM